Science Advances
AAAS

advances.sciencemag.org/cgi/content/full/4/8/eaat6224/DC1

Supplementary Materials for

Regulated nuclear accumulation of a histone methyltransferase times the onset of heterochromatin formation in *C. elegans* embryos

Beste Mutlu, Huei-Mei Chen, James J. Moresco, Barbara D. Orelo, Bing Yang, John M. Gaspar, Sabine Keppler-Ross, John R. Yates III, David H. Hall, Eleanor M. Maine, Susan E. Mango*

*Corresponding author. Email: smango@mcb.harvard.edu

Published 22 August 2018, *Sci. Adv.* **4**, eaat6224 (2018)
DOI: 10.1126/sciadv.aat6224

The PDF file includes:

Other Supplementary Material for this manuscript includes the following:

(available at advances.sciencemag.org/cgi/content/full/4/8/eaat6224/DC1)

Table S1 (Microsoft Excel format). Spectral counts and sequence coverage for proteins identified in the GFP immunoprecipitation and mass spectrometry experiment. Strains that lack GFP (N2), and contain MET-2::GFP or ZEN-4::GFP were processed in parallel.

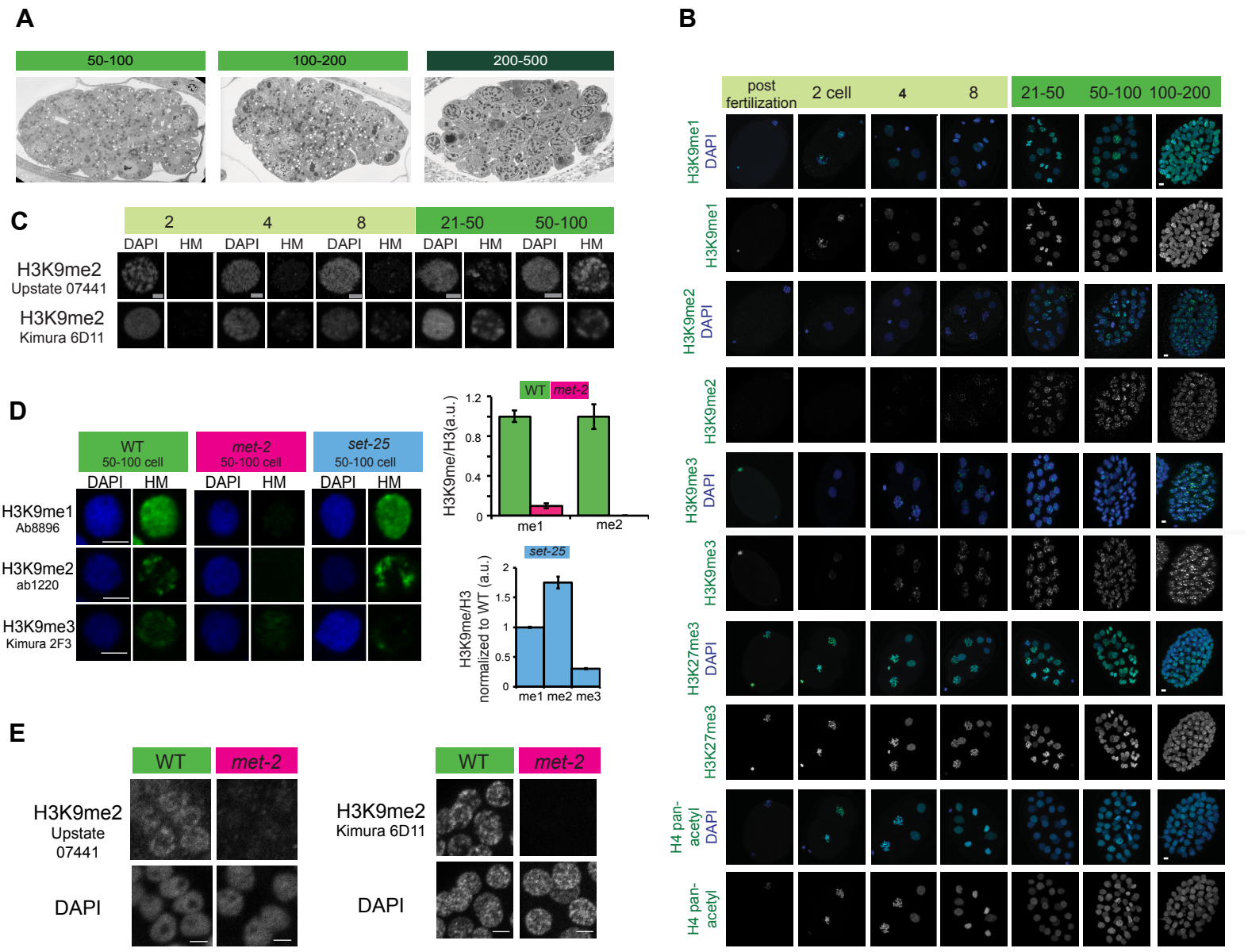

Fig. S1. Heterochromatin formation and establishment of H3K9me in WT embryos. (**A**) TEM single sections of whole embryos at designated stages. Each embryo is approximately 50µm long. (**B**) Whole embryos stained with H3K9me1/2/3, HK27me3 or H4 pan-acetylation at different stages of development (Scale bar 2 µm). (**C**) Representative single nuclei at designated stages showing H3K9me2 staining with two additional H3K9me2 antibodies: Upstate 07-441 and Kimura 6D11. (**D**) Antibody specificity for H3K9me2(ab1222) and H3K9me3 (Kimura 2F3): representative single nuclei at designated stages showing H3K9me staining in wild-type (green) vs. *met-2* (magenta) and *set-25* (blue) mutant embryos, Histone Modification (HM, green), DAPI (blue). H3K9me/Histone levels normalized to wild-type. Error bars denote standard error of the mean. (**E**) Antibody specificity for H3K9me2 (Upstate 07-441 and Kimura 6D11).

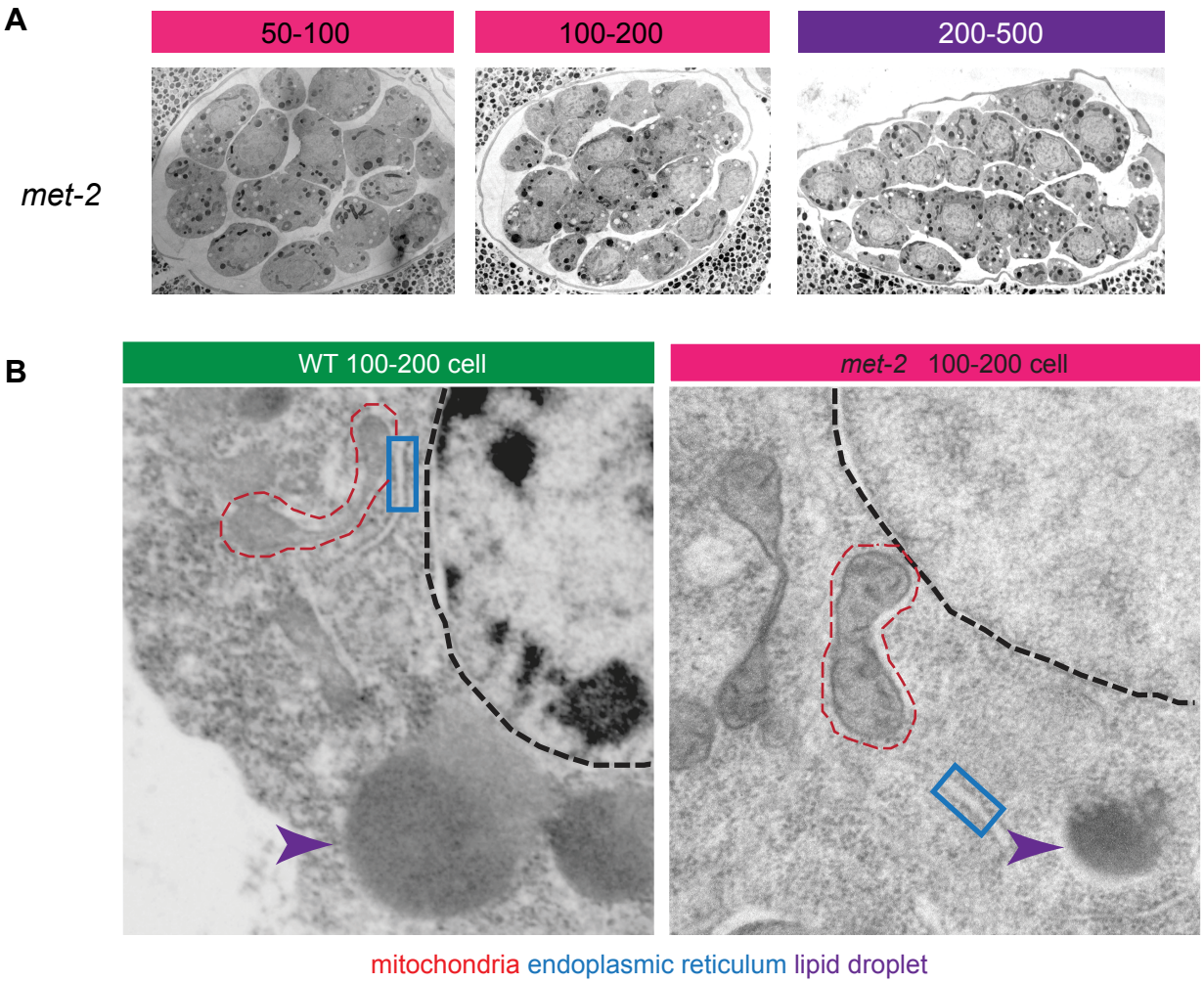

Fig. S2. Control for TEM conditions in WT versus *met-2* mutants. (**A**) TEM single sections of whole *met-2* embryos. Note the electron dense droplets in the cytoplasm vs. the electron lucent nuclei. (**B**) Cytosolic components in WT vs. *met-2* mutants by TEM. Mitochondria (red circle), endoplasmic reticulum (blue box), lipid droplet (purple arrowhead). Note the similar appearance of the cytosol vs. the different morphologies of the nuclei for wild-type vs *met-2.*

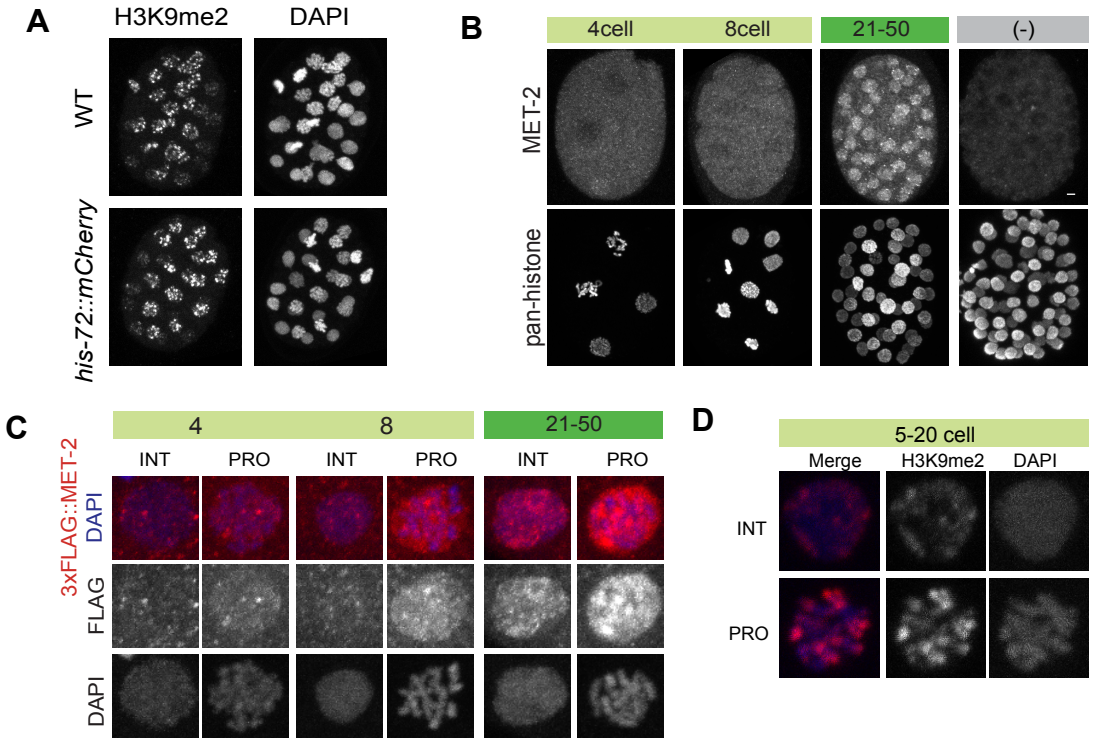

Fig. S3. MET-2 localization with additional reagents and during cell cycle. (**A**) H3K9me2 staining in wild-type vs. *his-72::mCherry* embryos showing that the mCherry tag doesn't interfere with H3K9me2. (**B**) Whole embryos stained with an antibody against endogenous MET-2 (raised against the first 17 amino acids of MET-2 protein) and pan-histone. (-) represents *met-2* mutants. Scale bar, 2 μm. (**C**) Representative single nuclei showing Crispr reporter 3xFLAG::MET-2 during interphase (INT) and prophase (PRO, Scale bar, 2 μm). (**D**) H3K9me2 levels in interphase (INT) and prophase (PRO) nuclei from the same embryo at the 15 cell stage.

A

	MET-2::GFP		(-)control	GFP control
	Spectral counts	Coverage	Spectral counts	Spectral counts
MET-2	895	36%	0	7
LIN-65	171	21%	0	0
B0336.5	8	21%	0	0
Histone H3	291	7%	0	0

B

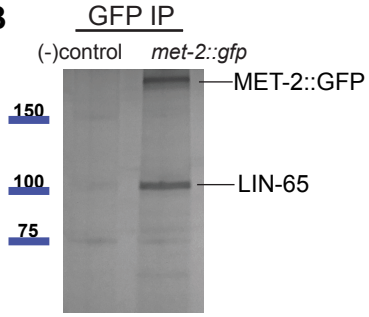

C

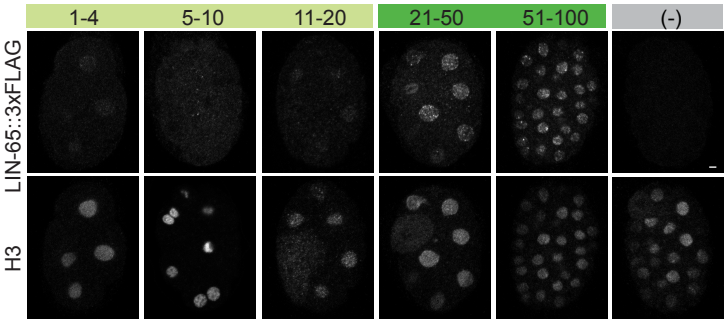

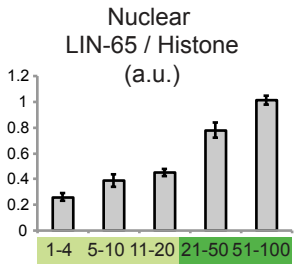

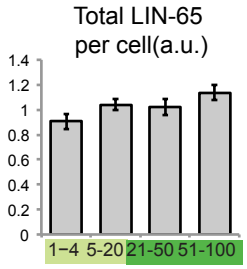

D

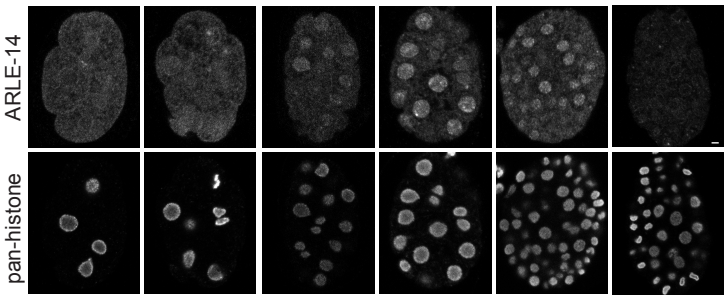

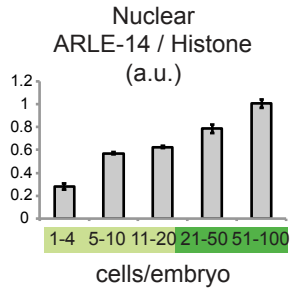

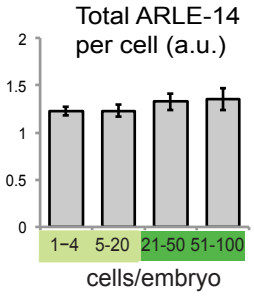

E

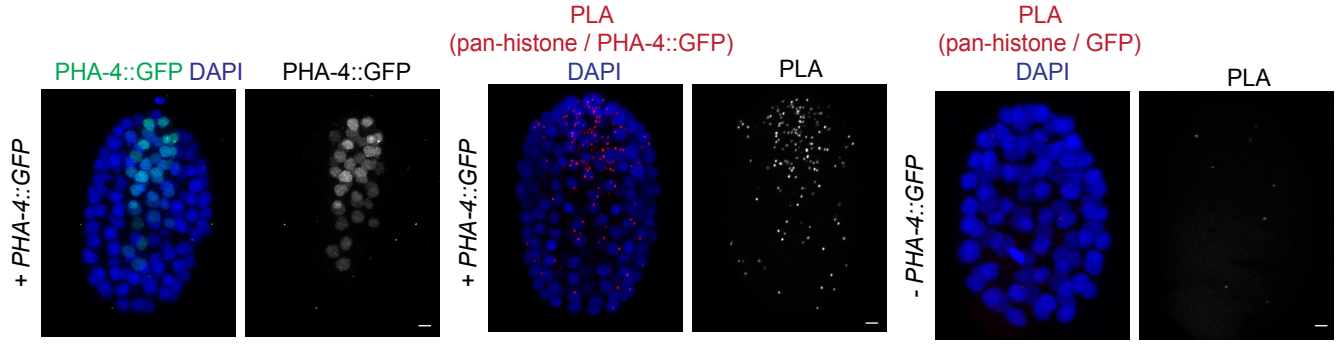

F

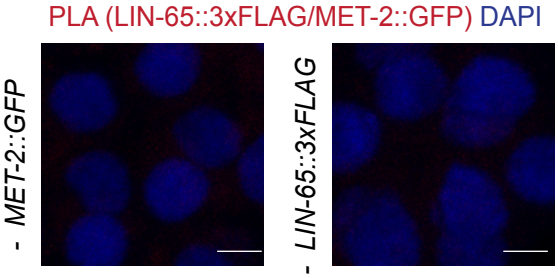

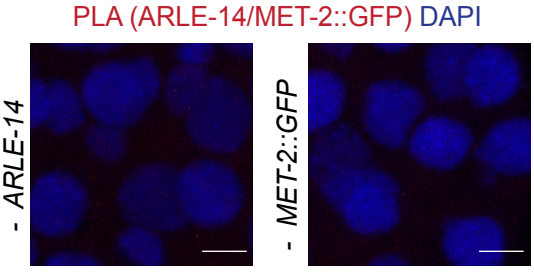

Fig. S4. Specificity controls for MET-2 coimmunoprecipitation and PLA. (**A**) Table showing spectral counts and peptide coverage after GFP IP-MudPIT MS for the following strains: *met-2::gfp*, wild-type (no GFP) and *zen-4::gfp* (GFP control). (**B**) Silver stain showing the 100 kDa LIN-65 band after MET-2::GFP IP, identified by cutting out the 100kDa band and Mass Spec. (**C** and **D**) Whole embryos showing LIN-65::3xFLAG (αFLAG antibody; C) and endogenous ARLE-14 (D) at different stages of embryonic development with a H3 or pan-histone co-stain (Scale bar, 2 μm). Quantitation of nuclear and total protein during embryogenesis, normalized to histone. (**E**) Left panel shows the staining pattern of transcription factor PHA-4::GFP (green) in whole embryos, with DNA (DAPI). The two panels on the right show PLA signal between GFP and pan-histone (red) with DNA (DAPI) in the following strains: *pha-4::gfp* or wild-type *N2* (no GFP -PHA-4::GFP) (Scalebar 2 μm). (**F**) Specificity controls for Fig. 4K. PLA for LIN-65::3xFLAG/MET-2::GFP (left panel) and MET-2::GFP/ARLE-14 (right panel) under conditions where individual proteins are depleted. (Scale bar 2 μm)

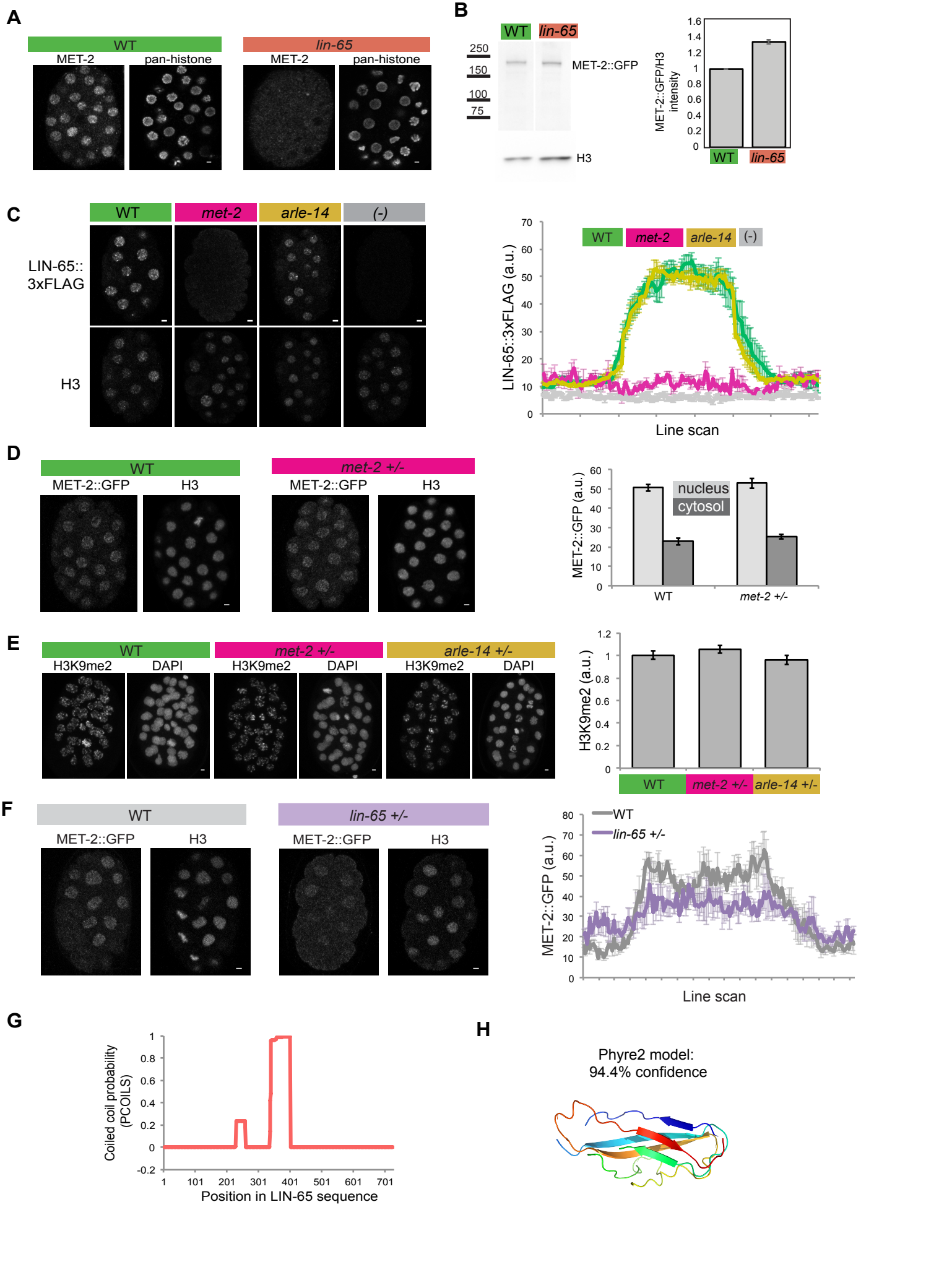
A
WT
lin-65
MET-2
pan-histone
MET-2
pan-histone
B
WT
lin-65
250
150
100
75
MET-2::GFP
H3
MET-2::GFP/H3 intensity
1.6
1.4
1.2
1
0.8
0.6
0.4
0.2
0
WT
lin-65
C
WT
met-2
arle-14
(-)
LIN-65::
3xFLAG
H3
LIN-65::3xFLAG (a.u.)
70
60
50
40
30
20
10
0
WT
met-2
arle-14
(-)
Line scan
D
WT
met-2 +/-
MET-2::GFP
H3
MET-2::GFP
H3
MET-2::GFP (a.u.)
60
50
40
30
20
10
0
nucleus
cytosol
WT
met-2 +/-
E
WT
met-2 +/-
arle-14 +/-
H3K9me2
DAPI
H3K9me2
DAPI
H3K9me2
DAPI
H3K9me2 (a.u.)
1.2
1
0.8
0.6
0.4
0.2
0
WT
met-2 +/-
arle-14 +/-
F
WT
lin-65 +/-
MET-2::GFP
H3
MET-2::GFP
H3
WT
lin-65 +/-
MET-2::GFP (a.u.)
80
70
60
50
40
30
20
10
0
Line scan
G
Coiled coil probability (PCOILS)
1
0.8
0.6
0.4
0.2
0
-0.2
1
101
201
301
401
501
601
701
Position in LIN-65 sequence
H
Phyre2 model:
94.4% confidence

Fig. S5. Further analysis of LIN-65 and dosage compensation for MET-2 protein. (**A**) Whole embryos stained with antibodies against endogenous MET-2 protein in wild-type (green) vs. *lin-65* (red) mutants, and co-stained for pan-histone. (**B**) MET-2::GFP IP and Western blot with GFP and histone antibodies in wild-type vs. *lin-65* embryonic extracts on the same gel. The lane between wild-type vs. *lin-65* is not shown. The graph shows pixel counts for the intensity of MET-2::GFP normalized to histone H3. Error bars denote standard error of the mean for N=2 experiments. (**C**) LIN-65::3xFLAG (αFLAG antibody) staining in wild-type vs. *met-2* and *arle-14* mutants. Line scan quantitation. Average of line scans across multiple nuclei are shown and error bars denote standard error of the mean. (**D**) MET-2::GFP levels in progeny of *met-2*(+/-) moms. Quantitation of MET-2::GFP signal intensity in the cytosol (dark grey) and the nucleus (light grey). Error bars denote standard error of the mean. (**E**) H3K9me2 levels in progeny of *met-2*(+/-) and *arle-14*(+/-) moms and quantified. Error bars denote standard error of the mean. (**F**) MET-2::GFP levels in WT vs. progeny of *lin-65*(+/-) heterozygous moms. Line scan quantitation showing mean accumulation of MET-2::GFP in wild-type (grey) or *lin-65*(+/-) (purple) embryos at the 21-50 cell stage. Average of line scans across multiple nuclei are shown and error bars denote standard error of the mean. (**G**) Coiled-coil probability across LIN-65 amino acid sequence predicted by PCOILS (https://toolkit.tuebingen.mpg.de/#/tools/pcoils). (**H**) Model structure of LIN-65 C-terminus predicted by Phyre2 (http://www.sbg.bio.ic.ac.uk/-phyre2/html/page.cgi?id=index). Full LIN-65 a.a. sequence was used as input for Phyre2.